JAST, Vol. 1, No. 1, pp 9–15

JAST
Journal of Aerospace Science and Technology

Numerical Investigation of Vortex Interaction in Pipe Flow

Prapat Suntivarakorn[1], Kazuo Matsuuchi[2]

To discover the nonlinear characteristics of pipe flow, we simulated the flow as a sum of many vortex rings. As a first step, we investigated the nonlinear interaction among a maximum of three vortex rings. The pipe wall was replaced by many bound vortices. A free vortex ring moves right or left according to the radius, and that of a particular radius keeps the initial position. The energy of a free vortex ring, except when it is close to a wall, coincides with that without boundaries. Two vortex rings of equal radii always show a repeated overtaking process. In the case of three vortex rings, they show a wide variety of behavior. For certain combinations of radii and the axial spaces among them, the motion, which seems to be very complex, is limited on a curved surface in three-dimensional space whose axes correspond to the three radii. It was found that this simplicity comes from the momentum conservation law, and also that its direction depends on the energy contribution calculated from free vortex rings. Our results elucidate the nonlinear behavior among many vortices.

NOMENCLATURE

English symbols

a	Radius of cross-section
a_0	Core radius
D	Diameter of pipe
E	Total energy
$\hat{E}$	Energy in a free space with no boundary
E_f	Energy obtained directly from free vortex rings
E_w	Energy evaluated from properties on pipe wall
E_{wv}	Energy evaluated from all vortices on pipe wall
$E(k^2)$	Complete elliptic integral of the first kind
$f(r)$	Cut-off factor
$K(k^2)$	Complete elliptic integral of the second kind
L	Length of pipe
P	Total momentum
P_f	Momentum due to free vortex rings
P_w	Momentum due to all bound vortices on pipe wall
r	Radial position
r_1	Distance of the nearest point on the vortex ring from the point (z, r)
r_2	Distance of the farthest point on the vortex ring from the point (z, r)
r_c	Cut-off radius
R	Radius of vortex ring
R_1	Radius of the first vortex ring
R_2	Radius of the second vortex ring
R_3	Radius of yhe third vortex ring
R_c	Critical radius for direction of motion
R_e	Equal radius of two vortex rings
R_p	Radius of pipe
t	Time
Δt	Time step
u	Axial velocity component
u_b	Axial induced velocity from all bound vortices on pipe wall

1. *Graduate School of Engineering, University of Tsukuba, Tsukuba, 305-8573, Japan.*
2. *Institute of Engineering Mechanics and Systems, University of Tsukuba, Tsukuba, 305-8573, Japan.*

u_s	Self-induced velocity
u_v	Axial induced velocity from other vortex
u_w	Axial velocity component on pipe wall
U	Total induced velocity
v	Radial velocity component
v_v	Radial induced velocity from other vortex
X	Position of vortex ring
z	Axial position
z_1	Axial position of the first vortex ring
z_2	Axial position of the second vortex ring
z_v	Axial position of vortex ring
Δz	Axial interval
Δz_L	Distance between the vortex ring of R_1 and R_2
Δz_R	Distance between the vortex ring of R_2 and R_3

Greek symbols

γ	Circulation of bound vortex on pipe wall
Γ	Circulation of vortex ring
ρ	Density

Subscripts

i	The i-th of free vortex ring
j	The j-th of bound vortex on pipe wall

INTRODUCTION

Since the famous experiment done by Reynolds in 1883, many studies on pipe flow have been done: nevertheless, many unsloved problems remain. In particular, the mechanism of transition from laminar to turbulent flow is not yet clear although many investigations have been made. For example, the necessary condition for the generation of puff in pipe flow is still not clear, despite the fact that the structure of puff was already clarified by many researchers. Matsuuchi et al. [1] studied the mechanism of puff in the initial stage of transition in pipe flow and found that the energy spectrum of the turbulence has the same slope, –3.3, in every condition for the generation of puff when a periodic disturbance was introduced by a loud speaker at a fixed Reynolds number of 2,200. Suntivarakorn and Matsuuchi [2] did an experiment to investigate the necessary condition for puff generation and confirmed that the energy spectrum of the turbulence has the universal slope of –3.3. However, the physical meaning of the universal slope of the energy spectrum is still unknown. The main reason for this is that strong nonlinearity takes place in the flow. To clarify the nonlinear characteristics, a discrete vortex method is applied. Many axisymmetric vortex rings are introduced to investigate vortex interaction. To understand the flow characteristics, interactions among many vortex rings have to be observed.

So far, most studies using the discrete vortex method have been devoted to unsteady jet flow. Morfey and Edwards [3] assumed an unsteady jet as a sum of many vortex rings. Furthermore, Acton [4] attemped to determine the numerical model for studying turbulent jet flow. The model they used was axisymmetric, invisicid and restricted to large-scale motions. By using this model, many features observed in real jet flow on the mixing region were demonstrated. This method was also applied to the axisymmetric jet issuing from a nozzle with a collar [5], and the flow around an axisymmetrical wing [6].

Many interesting applications have been used to observe several types of flows, but most of them were done from a practical point of view [7-10]. Only a few examples were applied to understand the unsteady behavior of pipe flow. Fineman and Chase [11] were the first to estimate numerically the energy of a vortex ring. Laulicht et al. [12] did an experiment to investigate the motion of a vortex ring in a tube. They found that the convection speed of the ring decreases as the diameter of the confining tube decreases. In recent years, Suntivarakorn and Matsuuchi [13] studied the mechanism of nonlinear interaction in pipe flow and tried to explain the meaning of the universal slope, –3.3. However, the problem of nonlinear characteristics in pipe flow is still unsolved.

Investigation of vortex interaction can lead us to an understanding of the nonlinear characteristics in pipe flow. The discrete vortex method is then applied. The statistical properties of velocity fluctuations, i.e., mean velocity and energy spectrum are estimated using this method. In particular, the energy spectrum can help us understand the mechanism of turbulence structure because it indicates the distribution of energy over different length scales.

The objective of this study was thus to understand the structure of pipe flow by considering it as a sum of many vortex rings. To clarify the unsteady features of pipe flow, the investigation of vortex interactions is important. As a first step, we investigated the nonlinear interaction among a maximum of three vortex rings and the interaction among vortex rings of equal circulation. Momentum and energy conservation in the present vortex ring system are also discussed to give a better understanding of the flow structure.

It was expected that the results would give a clear insight into the nonlinear behavior among many vortices in pipe flow. In a further study, many free vortex rings will be introduced in pipe flow which will imitate the disturbances in the laboratory experiment.

The flow in pipe is simulated using vortices and sources, and the velocity fluctuations and nonlinear vortex interaction are investigated at various downstream distances. The analysis of the energy spectrum will help us understand both the mechanism of the turbulence structure and the physical meaning of the universal slope, −3.3, in the spectrum.

METHOD OF CALCULATION

We assumed that flow is axisymmetric and used coordinates (z,r) in expressing the flow. The z-axis coincides with the axis of the pipe and r denotes the radial coordinate measured outwards from the axis. The pipe wall is replaced by 120 bound vortices which are placed at equal intervals ($\Delta z = 0.05$). The diameter of pipe $D = 1$ and its length $L = 6$. Free vortex rings with a constant circulation, $\Gamma = 1$, were introduced in pipe to investigate their interaction (See Figure 1). We calculated the velocity induced from the free vortex rings and bound vortices on the pipe wall, and determined the distribution of the circulation of the bound vortices on the pipe wall in such a way that the normal velocity component on the wall was zero. In discrete vortex representations of flows, unrealistic velocity fields are produced near the vortex elements. In particular, this causes undesired problems when two vortices come close together. The need for some smoothing of the discrete-vortex velocity field was first pointed out by Chorin and Bernard [14]; they proposed a cut-off for the velocity induced by each vortex. Then, Morfey and Edwards [3] introduced an appropriate cut-off to avoid unrealistic vortex configurations. They applied the cut-off, and showed that the momentum and energy conservations are maintained during the cut-off process. The same cut-off was also adopted in the present study.we will return to this point later. For later convenience, all quantities are made non-dimensional in terms of mean velocity and pipe diameter.

Induced Velocities

Seif-Induced Velocity

The motion of a free vortex ring of small cross-section is considered in an ideal fluid. The velocity of the ring normal to its plane, u_s, is given by

$$u_s = \frac{\Gamma}{4\pi R}(\ln\frac{8R}{a} - \frac{1}{4}). \tag{1}$$

Here R is the radius of the ring, and a is the radius of the cross-section [15, 16]. The radius a is governed by the relation $a_0^2 D/2 = a^2 R$, where a_0 is the core radius of the ring. This core radius was chosen to be 0.05D in view of the values of similar parameter employed by previous investigators [17, 18].

Induced Velocity from Other Vortices

Associated with each vortex ring, there occurs a velocity field whose axial and radial components at a point (z,r) are given by [19]

$$u_v = \Gamma R(RJ - rG), \tag{2}$$

$$v_v = \Gamma R(z - z_v)G. \tag{3}$$

Here Γ is the circulation of the vortex ring and z_v is the axial position of vortex ring. The quantities J and G are defined by

$$J = \frac{1}{\pi r_2^3}\frac{E(k^2)}{(1-k^2)} \tag{4}$$

$$G = -\frac{1}{\pi r_2^3 k^2}\left\{2K(k^2) - \frac{(2-k^2)}{(1-k^2)}E(k^2)\right\}. \tag{5}$$

Here $K(k^2)$, $E(k^2)$ are complete elliptic integrals of the first and second kind, respectively. The parameter k is defined as $k^2 = 1 - (r_1/r_2)^2$, where (r_1, r_2) are the distances of the nearest and farthest points on the vortex ring from the point (z,r) (see Figure 2).

Velocity Cut-off

An unwanted consequence of vortex interaction is the appearance of unrealistic induced velocities when they are close to each other. To ensure smoothing of the velocity field, without the strong mutual repulsions otherwise associated with close encounters, we followed Morfey and Edwards [3] in applying a cut-off factor expressed as

$$f(r_1) = \begin{cases} r_1^2/r_c^2, & r_1 < r_c \\ 1, & r_1 \geq r_c \end{cases} \tag{6}$$

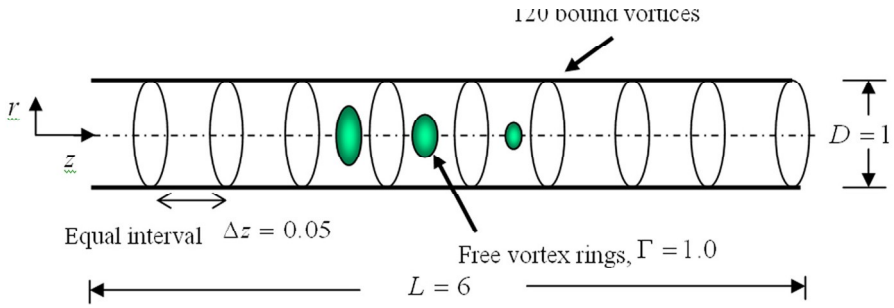

Figure 1. Vortex ring model.

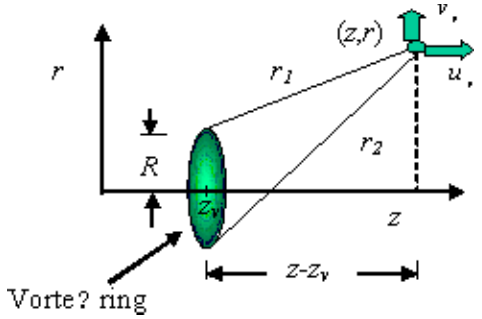

Figure 2. Sketch of velocity induced from a vortex ring.

to both the axial and radial induced velocity components, Eqs. (2) and (3). Here, r_c is a cut-off radius chosen as $r_c = 0.05$ [19].

Movement of Vortex Rings

Each vortex ring moves under the influence of all the other rings, and the subsequent position of each ring is calculated from the total induced velocity, $U(t)$. This velocity is the sum of the self-induced velocity (Eq. (1)), and the total induced velocities by all other vortices calculated from Eqs. (2) and (3). The new position of each vortex ring is given approximately by

$$X(t+\Delta t) = X(t) + \frac{3U(t) - U(t-\Delta t)}{2} \cdot \Delta t \qquad (7)$$

where $X(t)$ is the position of the vortex ring at time t, and Δt is the time step for computation, which is chosen as $\Delta t = 0.001$. Eq. (7) is an explicit formula for $X(t+\Delta t)$ in terms of $U(t)$ and $U(t-\Delta t)$ and it has a local truncation error proportional to $(\Delta t)^3$.

Momentum of the Vortex Ring System

We restricted our attention to an axisymmetric flow field in an inviscid fluid of constant density. The i-th vortex ring has radius R_i and circulation Γ_i. The flow field resulting from free vortex rings and bound vortices has a total momentum P, given by

$$P = \pi \sum \Gamma_i R_i^2 + \pi \sum \gamma_j R_p^2 \qquad (8)$$

where the summation extends over all the vortex rings, R_p is the radius of the pipe, and γ_j $(j = 1, 2, 3, \ldots, 120)$ is the distribution of circulation of bound vortices on the pipe wall. This momentum corresponds to the z-component of the real momentum. The total momentum in pipe flow consists of two kinds of momentum denoted in the first and second terms on the right-hand side of Eq. (8). The former is the momentum due to free vortex rings, P_f [15], and the latter is the momentum due to all the bound vortices on the pipe wall, P_w.

From a physical consideration, it is clear that the pipe flow has momentum conservation. When the pipe is long enough, vortex rings do not have any effects at either end of the pipe, and hence there is no influence of pressure at the ends. Since there is no external force and no axial pressure gradient on the pipe wall, the rate of change of momentum, $\partial P/\partial t$, must be zero. The momentum P is expected to be equal to zero because there was no initial impulsive force in the present calculation. It is also expected that the momentum P_f and P_w are independently conserved [13].

Energy of the Vortex Ring System

The total kinetic energy E of the present vortex ring system has two types of contributions as follows,

$$E = E_f + E_w \qquad (9)$$

where E_f is obtained directly from free vortex rings, which is given by [15]

$$E_f = 2\pi \sum \Gamma_i R_i (R_i u_i - z_i v_i) \qquad (10)$$

while E_w is the energy contribution evaluated from the properties on the pipe wall. In the above, Σ expresses the summation of all the free vortex rings and z_i, u_i, v_i are axial positions, axial and radial velocity components of the i-th vortex ring, respectively.

Assuming that there is no flow at either end of the pipe, we have for E_w

$$E_w = \frac{1}{2} \int 2\pi R_p^2 u_w^2 dz + E_{wv} \qquad (11)$$

where u_w is the axial velocity component on the pipe wall. The integration is carried out over the whole pipe length. The second term E_{wv} on the right-hand side corresponds to the direct contribution from all the vortices on the pipe wall. We calculated it by replacing R_i by R_p and setting $v_i = 0$ in Eq. (10).

RESULTS AND DISCUSSION

In this section, we investigate the vortex interaction when a maximum of three vortex rings exist in the pipe. We discuss the results of our calculations as three cases, cases A, B, and C corresponding to one, two and three vortex rings in the pipe.

Case A: One Vortex Ring

We assume that the circulation of clockwise-rotating vortices is negative and that of countericlockwise-rotating ones is positive. It is easy to see that circulation of the bound vortices on the pipe wall becomes negative for positive circulation of a free vortex ring. A free vortex ring has two types of induced velocities. One is a self-induced velocity, u_s, and the other one is the induced velocity from all bound vortices on the pipe wall, u_b. A Vortex ring of small radius moves right because $u_s > |u_b|$. The vortex ring of a particular radius keeps the initial position, i.e, the vortex ring does not move when $u_s = |u_b|$. This particular radius, R_c, is determined as 0.38 from the relation between two

functions u_s and $|u_b|$ of radius R [13]. A Vortex ring moves left when the radius is larger than R_c.

The obtained result shows that the velocity of a vortex ring moving in the forward direction decreases as its radius increases. This is similar to the experimental result of Laulicht et al. [12], who stated that the velocity of a vortex ring decreases with decreasing the diameter of the tube. Although Laulicht et al. investigated the velocity of a vortex ring by varying the diameter of the tube, their result is in good agreement with that of our calculated result by changing the radius of a vortex ring. We estimated the total energy E of the present vortex ring system in pipe flow and the energy $\hat{E}$ in a free space with no boundary. Both E and $\hat{E}$ can be calculated from Eq. (9), but the contribution for E_w must be zero for $\hat{E}$. Figure 3 illustrates the total energy E together with $\hat{E}$ as functions of radius R. The energy E_f and E_w are also shown separately in the same figure. When the radius of a vortex ring is smaller than 0.15, the total energy in pipe is only due to a free vortex ring ($E \approx E_f$), because there is no influence of vortices on the pipe wall ($E_w \approx 0$). The vortex ring moves like the one in a free space without a boundary, since E_f is equal to $\hat{E}$. It should be noted that the total energy E must be the sum of the energy E_f and E_w. When the radius of the vortex ring is larger than 0.15, E_f tends to be in negative and E_w increases from zero. Hence, E as a summation of E_f and E_w is always positive and agrees with $\hat{E}$. However, our calculation gives an incorrect estimate for E when $R > 0.45$ because the vortex ring is close to the wall; when the distance between the free vortex ring and the wall is smaller than the cut-off radius r_c (= 0.05), it gives an incorrect energy value. More noteworthy is that the vortex ring of a particular radius, which is at rest, is in agreement with the case when E_f is just zero. When E_f is positive, a vortex ring has a small radius and moves forwards. On the other hand, a vortex ring with large radius moves backwards for $E_f < 0$. The direction of motion depends on the sign of E_f. However, the total energy E is always positive whether the vortex ring moves forwards or backwards.

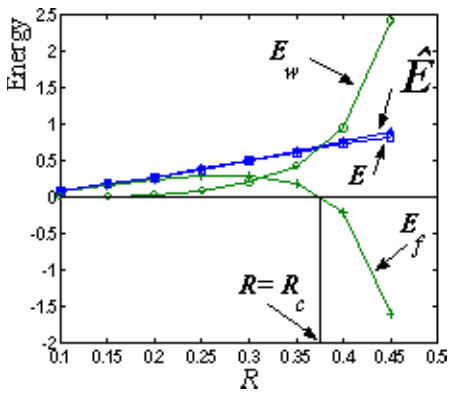

Figure 3. The energy of the vortex ring system.

Case B:Two Vortex Rings

When two vortex rings of equal radii R_e are located at $z_1 = 2.95$ and $z_2 = 3.0$, the direction of motion depends on their radii like case A. There are forward and backward motions. The rings always reveal an overtaking process. For example, when R_e is small, the axial induced velocity of the vortex ring at the rear is increased due to the front ring, while the front one is decreased by the induced velocity due to the ring behind it, and thus the ring passes through the front one. The overtaking process is repeated continously and both of the rings move forwards. When $R_e = 0.3775$, they also exhibit an overtaking process, but each ring can move only a limited distance. Figure 4 shows the trajectory of motion of two vortex rings. The abscissa and ordinate denote the position of the rear vortex ring, z_1, and that of the front one, z_2, respectively. At $t = 0$, the front vortex ring begins to move backwards from the initial position ($z_2 = 3.0$) and begins to turn back at $z_2 = 2.95$ to the original position. The motion is repeated with time. On the other hand, the vortex ring in the rear moves from $z_1 = 2.95$ and vice versa. The trajectory illustrates a closed orbit of the order (1) → (2) → (3) → (4) like a figure 8. Thus, two vortex rings move around only in a limited axial range whose length is 0.05. When the radii are larger than 0.3775, an overtaking process occurs as in the case of $R_e < 0.3775$, but both rings move backwards due to a strong velocity induced by wall vortices because of their large radii.

In general, the overtaking process of vortex rings can be seen from the ring smoke blowed from mouth of a smoker or chimney of a steam boat. However, the process is repeated only 2-3 times, and then the vortices disappear due to the influence of viscosity [20]. This is different from our inviscid result, in which the overtaking process was repeated continuously. Moreover, in free space with no boundary, the vortex rings move only in the forward direction [21], while the vortices in our calculation moved both forward and backward depending on their radii.

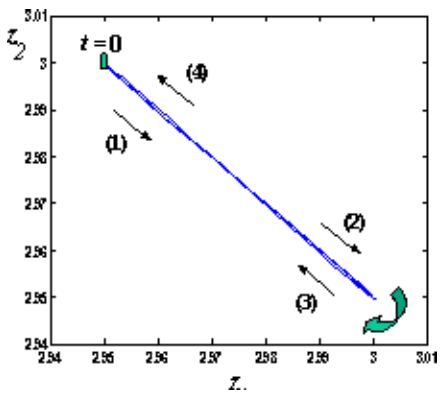

Figure 4. The trajectory of two vortex rings when $R_e = 0.3775$.

Case C: Three Vortex Rings

Three vortex rings of radii R_1, R_2 and R_3 are placed from left to right in this order. The distance between the vortex rings R_1 and R_2 is denoted by Δz_L, and that between the vortex rings R_2 and R_3 is Δz_R. Varying the radii and the distances, we have a wide variety of interactions. For example, when $R_1 = R_2 = 0.4$, $R_3 = 0.3$ and $\Delta z_L = \Delta z_R = 0.1$, the motion has an overtaking process continuosly with time in a complex manner (see Figure 5). The circulation of three vortex rings is assumed to be constant as $\Gamma_i = \Gamma = 1$. The momentum resulting directly from the three vortex rings, P_f, is proportional to the squared radii of the vortex rings. We calculated the momentum P_f for $0 \leq t \leq 25$, and obtained $0.41004 \pm 3.88x10^{-5}$ for P_f/π. This result means that the momentum P_f is conserved independently. The cut-off factor (see Eq. (6)) does not break the momentum conservation [3]. In Figure 6, we draw the variation of their radii in three-dimensional space (R_1, R_2, R_3). The trajectory seems to be very complex. To investigate this complicated structure, we utilized a Poincaré map. For example, Figure 7 shows points (R_2, R_3) where the tracjectory pierces the plane $R_1 = 0.36$. The points (R_2, R_3) are denoted

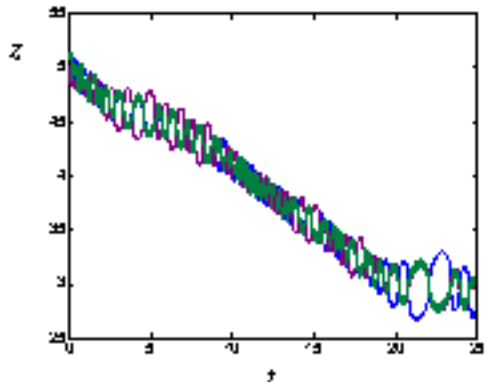

Figure 5. Movement of three vortex rings.

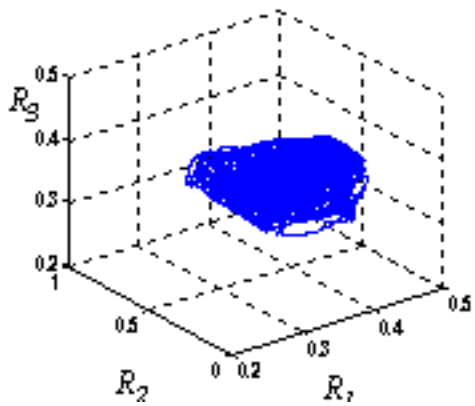

Figure 6. Motion of radii variation in three-dimensional space.

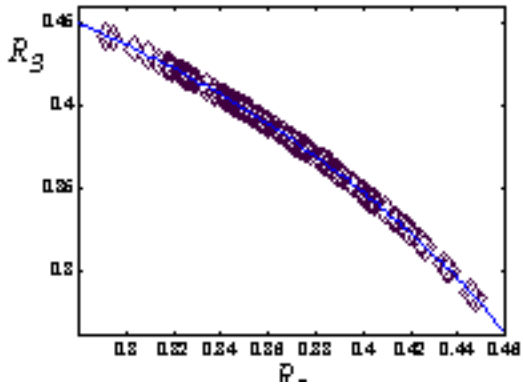

Figure 7. Momentum conservation of motion.

by the diamond symbol ($\Diamond$). In Figure 7, the solid line expresses the momentun conservation law, expressed as $R_3 = \sqrt{0.41 - 0.36^2 - R_2^2}$. It is clear that the symbol ($\Diamond$) coincides completely with the curve. Therefore, we conclude that three vortex rings move simply on the curved surface following the momentum conservation law.

Next, we estimated the energy using Eqs. (9)-(11). Figure 8 shows separately the variations of E, E_f, and E_w as functions of time. Two contributions E_f and E_w vary nonperiodically with time. The total energy E shows small fluctuations in some intervals of time due to the vortex interaction when the vortices come close together. The cut-off factor expressed in Eq. (6) breaks the energy conservation law. The energy is, however, approximately constant except for the intervals. From the discussion in Case A, it is plausible that the direction of motion is backward because E_f is negative. When Δz_L and Δz_R are larger than the above example, three vortex rings behave in a somewhat simpler manner like cases A and B.

CONCLUSION

We summarise our results as follows :

1. The motion of a vortex ring depends on its radius. We can divide the directions of motion into forward

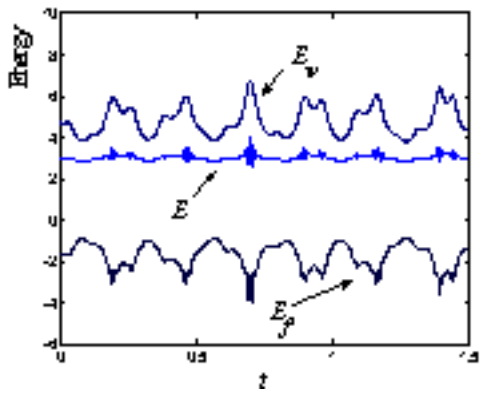

Figure 8. Conservation of energy.

and backward motions. The sign of E_f indicates the direction of motion. Positive and negative signs correspond to forward and backward directions, respectively.

2. The motion of two vortex rings of equal radii always shows an overtaking process and has two directions of motion similar to the results of a vortex ring.
3. According to the radii and the axial spaces among three vortex rings, they exhibit a wide variety of behaviors which are simple or complex.
4. Although the cut-off factor is invoked, it does not alter momentum conservation. On the other hand, in the case of energy, some small fluctuations occur in the total energy, but the energy conservation law is found to be applicable for energy estimation.

ACKNOWLEDGEMENTS

The useful advice and suggestions of all reviewers are gratefully acknowledged.

REFERENCES

1. Matsuuchi, K., Hakamaya, N. and Honma, T., "Initial stage of transition in a pipe and universality of turbulent structure", *Proc. 7th Asian Cong. Fluid Mech.*, Madras, PP 267-270(1997).
2. Suntivarakorn, P. and Matsuuchi, K., "Turbulence structure and chaotic phenomenon in the initial stage of transition in pipe flow", *Proc. 9th Int. Symp. on Flow Visualization*, Scotland, 291, ((2000)).
3. Morfey, C.L. and Edwards, A.V.J., "Energy and momentum constraints on the use of a cutoff in lumped-vortex flow models", *ISVR Technical Memorandum*, 587, (1978).
4. Acton, E., "A model of large eddies in an axisymmetric jet", *J. Fluid Mech.*, **98**, PP 1-31(1980).
5. Shimizu, S., "Simulation of axisymmetric jet issuing from a nozzle with collar. Trans. JSME", *J. Fluid Mech.*, In Japanese, **Series B, 59**, PP 151-156(1993).
6. Hamano, K., Koso, T., Mizuno, A. and Ohashi, H., "Numerical analysis by discrete vortex method of the flow field of a jet with Thurst-Augmenter", *Proc. 10th Symp. Computational Fluid Dynamics*, In Japanese, 587, PP 362-363(1996).
7. Lewis, R.I., *Vortex element methods for fluid dynamic analysis of engineering systems*, Cambridge University Press, (1991).
8. Gibson, I.S., "Theoretical studies of tip clearance and radial variation of blade loading on the operation of ducted fans and propellers", *J. Mech. Eng. Sci.*, **16**(6), PP 367-376(1974).
9. Y. Yonezawa and T. Tsukiji, "Numerical analysis of a flow in three-dimensional poppet valve by discrete-vortex method", *Research Compilation of Ashikaga Institute of Technology*, In Japanese, **20**, PP 57-61(1994).
10. Miura, Y., Nakanishi, Y. and Kamemoto, K., "Numerical simulation of flow behind a backward facing step by the vortex method", *Proc. 7th Symp Computational Fluid Dynamics*, Tokyo, (In Japanese), PP 617-620(1993).
11. Fineman, J.C. and Chase, C.E., "Energy of a vortex ring in a tube and critical velocities in liquid helium II", *Phys. Rev.*, **129**(1), PP 1-7(1963).
12. Laulicht, B., Bohl, D. and Koochesfahani, M.M., "Vortex ring in a tube", *Bull. Am. Phys. Soc.*, **43**(9), PP 2010-2011(1998).
13. Suntivarakorn, P. and Matsuuchi, K., "Vortex-vortex interaction in pipe flow", *J. Japan Soc. Fluid Mech.*, In Japanese, **20**(1), PP 68-77((2002)).
14. Chorin, A. J. and Bernard, P. S., "Discretization of a vortex sheet, with an example of roll-up", *J. Comput. Phys.*, **13**, PP 423-429(1973).
15. Lamb, H., *Hydrodynamics*, 6th Ed.Ed., Cambridge University Press, (1975).
16. Saffman, P.G., "The velocity of viscous vortex rings.", Stud. Appl. Math., PP 371-380(1970).
17. The Japan Society of Mechanical Engineers, *Fundamentals of computational fluid dynamics*, Corona Publishing, (1988).
18. Kiya, M., Sasaki, K. and Arie, M., "Discrete-vortex simulation of a turbulent separation buble", *J. Fluid Mech.*, **120**, PP 219-244(1982).
19. Edwards, A.V.J. and Morfey, C.L., "A computer simulation of turbulent jet flow.", *Computers and Fluids*, **9**, PP 205-221(1981).
20. Maxworthy, T., "The structure and stability of vortex rings", *J. Fluid Mech.*, **51**(part 1), PP 15-32(1972).
21. Oshima, Y., Noguchi, T. and Oshima, K., "Numerical study of interaction of two vortex rings", *Fluid Dynamics Research*, **1**, PP 215-227(1986).